Strand and Cell Type-specific Function of microRNA-126 in Angiogenesis

Qinbo Zhou[1], Chastain Anderson[1], Jakub Hanus[1], Fangkun Zhao[1], Jing Ma[1], Akihiko Yoshimura[2] and Shusheng Wang[1,3]

[1]Department of Cell and Molecular Biology, Tulane University, New Orleans, Louisiana, USA; [2]Department of Microbiology and Immunology, Keio University School of Medicine, Shinjuku-ku, Tokyo, Japan; [3]Department of Ophthalmology, Tulane University, New Orleans, Louisiana, USA

microRNAs or miRs have been shown to be pivotal modulators of vascular development. The strand and cell type-specific function of miR-126 in angiogenesis, especially pathological angiogenesis, remains poorly defined. We characterized the retinal vascular phenotype of *miR-126*$^{-/-}$ mice, and tested the function of miR-126 strands (miR-126-3p and -5p) using *in vitro* angiogenesis models and a mouse model of neovascular age-related macular degeneration. We found that miR-126 is critical for retinal vascular development but has dual function in pathological angiogenesis. *miR-126*$^{-/-}$ mice showed defective postnatal retinal vascular development and remodeling, which is partially rescued by genetic knockout of its target gene *Spred-1*. Surprisingly, either silencing miR-126-3p by LNA-antimiR or overexpressing miR-126-3p by miRNA mimic repressed laser-induced choroidal neovascularization. To dissect the underlying mechanism, we found in endothelial cells, silencing of miR-126-3p repressed angiogenesis, while overexpression of miR-126-5p enhanced angiogenesis. However, in retinal pigment epithelial cells, miR-126-3p repressed vascular endothelial growth factor (VEGF-A) expression via a novel mechanism of regulating αB-Crystallin promoter activity and by directly targeting VEGF-A 3′-untranslated region. These findings provide first genetic evidence that miR-126 is required for the development of different retinal vascular layers, and also uncover a strand and cell type-specific function of miR-126 in ocular pathological angiogenesis.

Received 17 March 2016; accepted 11 May 2016; advance online publication 21 June 2016. doi:10.1038/mt.2016.108

INTRODUCTION

The retina has been an excellent model to study developmental and pathological angiogenesis. Vascularization of the mouse outer retina occurs through two waves of angiogenesis after birth, when endothelial cells (ECs) sprout from the central retinal artery to the peripheral region and then to the intermediate and deep layers of the retinal vascular plexus.[1,2] Pathological angiogenesis in the eye is the most common cause of blindness at all ages and underlies conditions such as retinopathy of prematurity in children, diabetic retinopathy in young adults and age-related macular degeneration (AMD) in the elderly. AMD is a degenerative disease of the retina and the leading cause of blindness among the elderly.[3] Neovascular (or wet) AMD, which accounts for the majority of acute vision loss in AMD, is characterized by choroidal neovascularization (CNV), a process involving abnormal growth of blood vessels from the choroid into the retina. Vascular endothelial growth factor (VEGF), which is highly expressed in the retinal pigment epithelial (RPE) cells in the eye, is a major cytokine driving neovascularization and vascular permeability during CNV. Several FDA-approved anti-VEGF agents, including Macugen, Lucentis and Eylea, are the current mainstay for wet AMD treatment.[4–6] Although anti-VEGF agents have markedly improved the clinical outcome of wet AMD, they have been unable to induce complete CNV regression, and only 30–40% of individuals experienced vision improvement after treatment.[7,8] Developing novel alternative approaches to complement anti-VEGF therapy is becoming increasingly imperative.

microRNAs (miRNAs, or miRs) represent a group of small noncoding RNAs (~22 nucleotides in size) that repress multiple target genes and are implicated in numerous diseases, including cardiovascular disease and cancer.[9,10] An increasing list of miRNAs, termed "angiomiRs", has been shown to regulate angiogenesis cell autonomously or noncell autonomously.[11] Specifically, several miRNAs, including miR-23/miR-27, miR-21, and miR-24 have shown to be important regulators of CNV in a laser injury-induced CNV model.[12–14] We and others have demonstrated that miR-126, one of the highly expressed miRNAs in ECs, is required for angiogenesis and vascular integrity *in vivo*.[15–17] Consistently, silencing of miR-126 by antagomiR impares ischemia-induced angiogenesis.[18] miR-126 is located in the intron 7 of the host gene epidermal growth factor-like protein 7 (*Egfl7*) in mice. In a recent study, overexpression of miR-126-5p has been shown to promote EC proliferation and limits atherosclerosis.[19] The action of miR-126-3p in ECs is known to be mediated by promoting MAP kinase and PI3K signaling in response to growth factors, through targeting negative regulators of the pathways, including the Sprouty-related protein *Spred-1* and phosphoinositol-3 kinase regulatory subunit 2 (*PIK3R2/p85-β*)[15–17,20]; while the action of miR-126-5p in promoting EC proliferation is through targeting *Dlk1*, a noncanonical NOTCH1 inhibitor.[19] However,

Correspondence: Shusheng Wang, Tulane University, 2000 Percival Stern Hall, 6400 Freret Street, New Orleans, Louisiana 70118, USA. E-mail: swang1@tulane.edu

there were also studies showing that miR-126 is downregulated in many cancer lines and restoration (or overexpression) of miR-126 inhibits tumorigenesis and cancer cell invasion by targeting VEGF, PIK3R2, and adapter protein CRK.[21–25] In the context of neovascularization, overexpression of miR-126 has been shown to inhibit ischemia-induced retinal neovascularization.[26] These conflicting results necessitate a thorough functional study of miR-126 in angiogenesis.

We hypothesize that the discrepancy in different miR-126 studies could be explained by the cell type and strand-specific function of miR-126. In the current study, we aimed to address the cell type and strand-specific function of miR-126 in angiogenesis using models of developmental and pathological angiogenesis. Using a *miR-126*$^{-/-}$ mouse model, we identified a critical role for *miR-126/Spred-1* genetic pathway in the development of retinal vascular layers. Using a laser-induced CNV pathological angiogenesis model, we found that silencing of miR-126-3p by locked nucleic acid (LNA)-modified anti-miR or overexpression of miR-126-3p by miR-126-3p mimic repressed laser-induced CNV *in vivo*. To dissect its underlying mechanism, we found that miR-126 has cell type and strand specific function in angiogenesis. This study may be instrumental for developing miR-126-based therapy for angiogenesis-related diseases.

RESULTS

EC-enriched miR-126 expression and *Egfl7/miR-126* promoter activity in mouse eye

We and others have established a critical role for miR-126 in regulating vascular integrity and angiogenesis.[15–17] To further study the function of miR-126 in developmental and pathological angiogenesis, we first examined miR-126 expression in the retina by qPCR and by *in situ* hybridization (ISH) using Dig-labeled LNA modified miR-126-3p probe. By qPCR, miR-126-3p expression was increased in the eyes of postnatal (P) day 12 mice compared to that in P1 mice, which was further increased in P28 eyes (**Supplementary Figure S1**). This is consistent with the increased retinal vasculature during postnatal mouse development. By ISH, miR-126-3p expression was restricted to the vessels in both retina and choroid of mice (**Figure 1a** (A–C)). As control, miR-126-3p was not detected in *miR-126*$^{-/-}$ mouse retina, confirming the specificity of the probe (**Figure 1a** (D)). miR-126 is located in the intron of *Egfl7* gene, and we have identified a 5.5kb promoter driving EC-enriched *Egfl7/miR-126* expression.[17] We generated stable mouse lines that express β-galactosidase (LacZ) reporter under the control of the *Egfl7/miR-126* promoter (p-miR-126-LacZ mice; **Figure 1b**). LacZ and platelet endothelial cell adhesion molecule 1 (PECAM-1) antibody co-staining revealed strong miR-126 promoter activity in the ECs of the ocular tissues, including the retina and choroid (**Figure 1c**). Taken together, our data

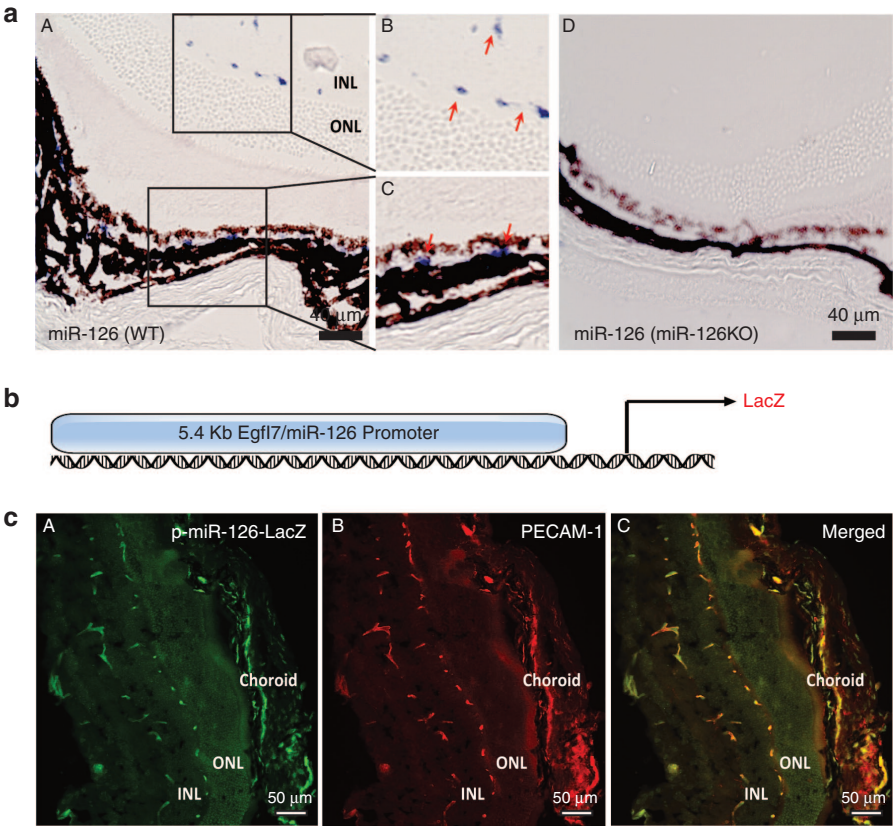

Figure 1 EC-enriched miR-126 expression and *miR-126/Egfl7* promoter activity in the mouse retina. (**a**) Section *in situ* detection of miR-126-3p expression in retinal and choroid vasculature in WT mice (**A**). (**B**) and (**C**) are the magnification of the boxed regions in (**A**). *miR-126*$^{-/-}$ retina (**D**) was used as negative control for specificity of the probe. INL: inner nuclear layer. ONL: outer nuclear layer. Scale bar equals to 40 μm. (**b**) Schematic *pmiR-126/Egfl7-LacZ* construct containing LacZ reporter driven by a 5.4kb *miR-126/Egfl7* promoter. (**c**) LacZ and PECAM-1 co-staining of the retina cross sections in 4-week old *pmiR-126/Egfl7-LacZ* transgenic mice showing co-localized expression of LacZ and PECAM-1 in the retinal and choroidal vasculature. (**A**) LacZ antibody staining; (**B**) PECAM-1 staining; (**C**) Merged picture. Scale bar equals to 50 μm.

confirmed that miR-126-3p expression is EC-enriched in ocular vasculature, and the 5.4 kb *Egfl7/miR-126* promoter is sufficient to drive EC-enriched gene expression in the eye.

Defective retinal vascular development in *miR-126*$^{-/-}$ mice and its rescue by *Spred-1* deletion

We took advantage of the partial lethality of *miR-126*$^{-/-}$ mice, and used the surviving knockout mice to study the role of miR-126 in retinal vascular development. Vascularization of the retina in *miR-126*$^{-/-}$ mice was greatly compromised compared to the wild type (WT) controls (**Supplementary Figure S2a**). The vascular coverage of the superficial layer of the retina was ~30% less in the P6-P8 *miR-126*$^{-/-}$ retina compared to the WT controls as shown by intracellular adhesion molecule 2 (ICAM-2) staining and quantification (**Supplementary Figure S2b**). Astrocyte development was normal as shown by glial fibrillary protein staining, suggesting the retinal vascular defects in *miR-126*$^{-/-}$ mice was not secondary to defective astrocyte recruitment (**Supplementary Figure S2c**). By P10, the intermediate and deep layers of the retinal plexus are formed and connected (**Figure 2a** (A, C, E)). However, very few retinal vessels sprouted into the intermediate layers and the deep layer in *miR-126*$^{-/-}$ mice as shown by confocal imaging of retinal layers and 3-D reconstruction (**Figure 2a** (B, D and F)). This defective retinal vasculature persisted in adult *miR-126*$^{-/-}$ mice (**Figure 2b**). Notably, in the superficial layer, there was much less branching in the *miR-126*$^{-/-}$ retinas compared to the numerous tree-branch like vessel structures in the adult WT retinas. These results indicate a requirement for miR-126 in the development of retinal vascular layers.

We and others have shown that *Spred-1* is a major miR-126-3p target gene in ECs.[15–17,20] To genetically establish *Spred-1* as a major miR-126-3p target gene, we asked whether the *miR-126*$^{-/-}$ phenotype can be rescued by simultaneous knockout of *Spred-1*. *Spred-1*$^{-/-}$ mice are viable and without obvious phenotype.[27] We generated *Spred-1*/*miR-126* double knockout mice and compared their retinal vascular development with *miR-126*$^{-/-}$ mice, and found that the defective sprouting of the retinal vessels into the deep retinal layer in the *miR-126*$^{-/-}$ mice was partially rescued in the *Spred-1*/*miR-126* double knockout mice (**Figure 2c**). Together with our previous data and others, this provides strong support that *Spred-1* is a bona fide miR-126-3p target *in vivo*.[15–17,20]

Repression of CNV by LNA-modified anti-miR-126-3p

To explore miR-126 function in pathological angiogenesis, we found miR-126-3p expression in the choroid was significantly upregulated at 14 days after laser injury, consistent with increasing CNV in this model[28] (**Supplementary Figure S3a**). This suggests an involvement of miR-126 in CNV. To directly test miR-126-3p/5p function in CNV, LNA modified anti-miR-126-3p/5p (Exiqon, Woburn, MA) was used to knockdown miR-126 in the choroid.[29] LNA anti-miR-126-3p, anti-miR-126-5p, or a scramble control, was injected subretinally into the eye immediately following laser injury in three locations and at post injury day 3 and 7. LNA-anti-miR-126-3p and anti-miR-126-5p specifically silenced miR-126-3p and miR-126-5p expression in the eye at 7 days after injection (**Supplementary Figure S3b**). Of note, these LNA-antimiRs for *in vivo* injection were designed to be less than 17 nucleotides in length, therefore avoiding potential generic siRNA-like effects of anti-miR in suppressing CNV.[30] CNV area was quantified after ICAM-2 staining of the lesion at 14 days after injury. miR-126-3p silencing significantly repressed CNV area by about 50% compared to scramble control (2,413 ± 481 μm^2 (N = 13) in the control, versus 1,094 ± 210 μm^2 (N = 12) in the anti-miR-126-3p group, $P < 0.05$; **Figure 3a**,**b**), suggesting that miR-126-3p is required for modulating neovascularization in the choroid. However, silencing of miR-126-5p did not significantly impact CNV (2,413 ± 481 μm^2 (N = 13) in the control, versus 2,229 ± 405 μm^2 (N = 12) in the anti-miR-126-5p group), indicating differential requirement for miR-126-3p and miR-126-5p in CNV.

To further confirm the differential requirement for miR-126-3p and -5p in angiogenesis, an EC-fibroblast co-culture assay was performed.[31] When ECs are cultured on the top of a confluent fibroblast cell layer, ECs will form three-dimensional vascular tubules resembling capillaries as stained by antibody to PECAM-1 (**Figure 3c**). Compared to the scramble control, anti-miR-126-3p but not -5p significantly repressed the formation of vascular tubules at 11 days after co-culture by PECAM-1 staining and vessel density quantification (**Figure 3c**,**d**), consistent with our *in vivo* laser-CNV study. We therefore conclude that miR-126-3p but not miR-126-5p is required for proper angiogenesis *in vitro* and *in vivo*.

Overexpression of miR-126-3p by mimics represses laser-induced CNV *in vivo*

To determine whether miR-126-3p overexpression promotes pathological angiogenesis, miR-126-3p mimic (Genepharma) was injected subretinally after laser injury, and CNV was quantified 2 weeks later. FAM-labeled miRNA mimic was first used to visualize the distribution of miRNA mimics after injection. FAM-labeled miRNA mimic was successfully delivered into the injured region and partially overlapped with the Isolectin-B4-stained vasculature (**Figure 4a**). Of note, significant FAM-labeled mimic was also present in the RPE layer in the injured region. By qRT-PCR, 1ul of miR-126-3p mimic (200 ng/μl) injection led to ~11-fold increase in miR-126 expression in the posterior eye cup, indicating efficient delivery of miRNA mimics into the choroid *in vivo* (**Figure 4b**). CNV area quantification revealed that miR-126-3p mimic led to ~60% decrease in CNV (3,214 ± 581 μm^2, N = 18 in the mimic control, versus 1,179 ± 188 μm^2, N = 27 in miR-126-3p mimic injected samples; **Figure 4c**,**d**). Decreased neovascularization of the choroid was also confirmed by ICAM-2 staining of frozen sections (**Figure 4c**). We also tested the effect of miR-126-5p mimic in laser-induced CNV, and found miR-126-5p mimic significantly but mildly enhanced laser-induced CNV compared to the control mimic (2,643 ± 169 μm^2, N = 16 in the mimic control, versus 3,206 ± 185 μm^2, N = 19 in miR-126-5p mimic injected samples, $P < 0.05$, **Supplementary Figure S4A,B**). Our data revealed that miR-126-3p overexpression is sufficient to repress CNV *in vivo*.

Overexpression of miR-126-3p in ECs does not promote angiogenesis

Given the surprising results that miR-126-3p mimic represses CNV *in vivo*, we asked whether miR-126-3p mimic directly represses EC proliferation and migration. BrdU incorporation assay and scratch wound assay were performed to test the effect of miR-126-3p or -5p mimic on EC proliferation and migration.

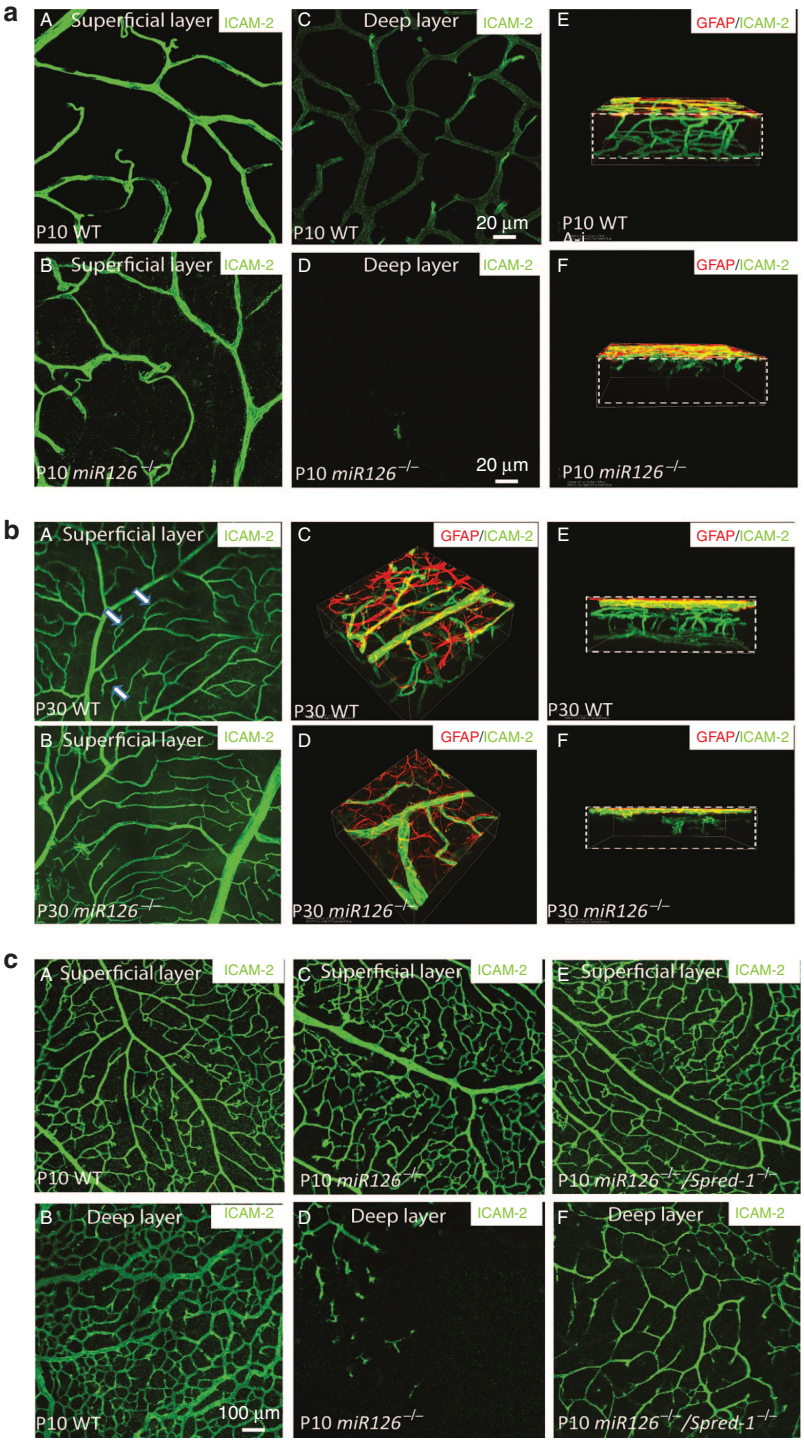

Figure 2 Retinal vascular phenotype in *miR-126*$^{-/-}$ mice and its rescue by *Spred-1* knockout. (**a**) Representative ICAM-2 (green) and glial fibrillary protein (GFAP) (red) staining of a postnatal day 10 (P10) WT and a *miR-126*$^{-/-}$ flatmount retina showing defective retinal vascular sprouting in *miR-126*$^{-/-}$ mice. **A**, **C**, and **E** are ICAM-2 staining of the retinal superficial layer, deep layer, and 3-D reconstruction of the retinas in WT mice; while **B**, **D** and **E** are the ICAM-2 staining of the corresponding regions in *miR-126*$^{-/-}$ mice. Boxes in **E** and **F** indicate the retina with different layers visualized. Scale bar equals 20 μm. (**b**) GFAP and ICAM-2 co-staining of the P30 WT and a *miR-126*$^{-/-}$ flatmount retina showing that retinal vascular sprouting is not recovered in P30 *miR-126*$^{-/-}$ mice. **A** and **B** show the ICAM-2 staining of the superficial layer retinas. Arrows indicate significantly more branches in the WT mice compared to the *miR-126*$^{-/-}$ mice. **C** to **F** are 3D reconstruction of the P30 retinas from different angles after ICAM-2/GFAP staining. (**c**) Partial rescue of retinal angiogenic phenotype in *miR-126*$^{-/-}$ mice by knockout of its target gene *Spred-1*. ICAM-2 staining of the superficial (**A**, **C**, **E**) and deep layer (**B**, **D**, **F**) of P10 retinas from different genotypes indicated was shown. Scale bar equals 100 μm.

Under starvation condition, miR-126-5p but not miR-126-3p significantly increased EC proliferation (**Figure 5a**). With VEGF treatment, miR-126-3p mildly but significantly repressed EC proliferation, but miR-126-5p significantly enhanced EC proliferation by ~70%. Similarly, miR-126-5p but not miR-126-3p significantly enhanced VEGF-induced EC migration in a scratch

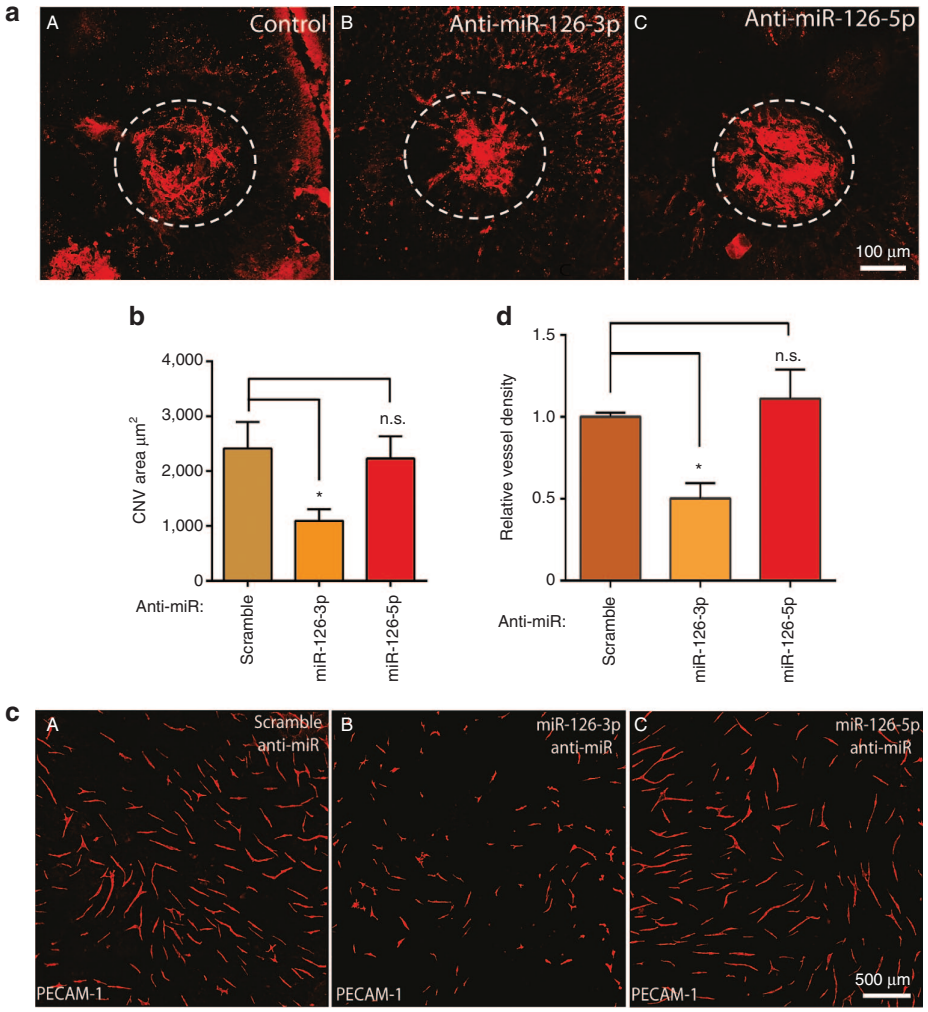

Figure 3 Repression of laser-induced CNV and angiogenesis by miR-126-3p. (**a**) Representative images of RPE/choroid flatmount after ICAM-2 staining showing repression of laser-induced CNV by LNA-antimiR-126-3p but not LNA-antimiR-126-5p. Scale bar equals 100 μm. Circled regions are the CNV areas. (**A**) Control; (**B**) LNA-antimiR-126-3p; (**C**) LNA-antimiR-126-5p. (**b**) Quantification of CNV area in **a**. N.S., not significant; *, $P < 0.05$. (**c**) Representative images of vessel-like structures as stained by PECAM-1 in an EC-fibroblast co-culture assay after silencing of miR-126-3p or miR-126-5p in ECs. (**A**) Control; (**B**) LNA-antimiR-126-3p; (**C**) LNA-antimiR-126-5p. Scale bar equals 500 μm. (**d**) Quantification of vessel density EC-fibroblast co-culture assay after silencing of miR-126-3p or miR-126-5p. *, $P < 0.05$; N.S., not significant.

wound assay (Figure 5b,c). Of note, in the EC migration assay, 5-fluorouracil was added to the medium before VEGF treatment to prevent EC proliferation, therefore ruling out the confounding effect of cell proliferation on cell migration. We also confirmed our results in an EC-fibroblast co-culture angiogenesis assay, and found that miR-126-5p but not miR-126-3p mimetics enhanced angiogenesis as quantified by vessel density (Figure 5d,e). We found miR-126-5p but not miR-126-3p mimic significantly represses *DLK1* expression, consistent with a recent report showing that miR-126-5p enhances angiogenesis by targeting Dlk1 (**Supplementary Figure S5**).[19] These results suggest that the repressive effect of the miR-126-3p mimic in CNV *in vivo* is not caused by its effect in ECs.

Repression of VEGF expression by miR-126-3p in RPE cells

Based on the results above, we hypothesized that miR-126-3p mimic represses CNV via an indirect mechanism. Although miR-126 is required for VEGF signaling in ECs, its overexpression could repress VEGF expression in other cell types, highlighting the cell type-specific function of this miRNA.[15–17,20,23,26] We hypothesized that the differential effect of miR-126 strands overexpression/knockdown in different cell types could be explained by differential expression of VEGF and signaling pathways in different cells. We have shown that miRNA mimic is distributed in both choroidal vasculature and its neighboring RPE cells after subretinal delivery (Figure 4a). We found that RPE cells express much higher level of VEGF protein but much lower level of miR-126-3p and -5p than ECs (Figure 6a,b). When miR-126-3p was overexpressed in ARPE-19 cells by miR-126-3p mimic, VEGF-A protein level was significantly reduced as shown by ELISA analysis; while miR-126-3p knockdown led to a mild but significant upregulation of VEGF-A protein expression, probably due to the low endogenous miR-126 level in RPE cells (Figure 6c,d). The repression of VEGF-A by miR-126-3p was also verified by Western blot analysis (Figure 6e). Of note, miR-126-5p didn't

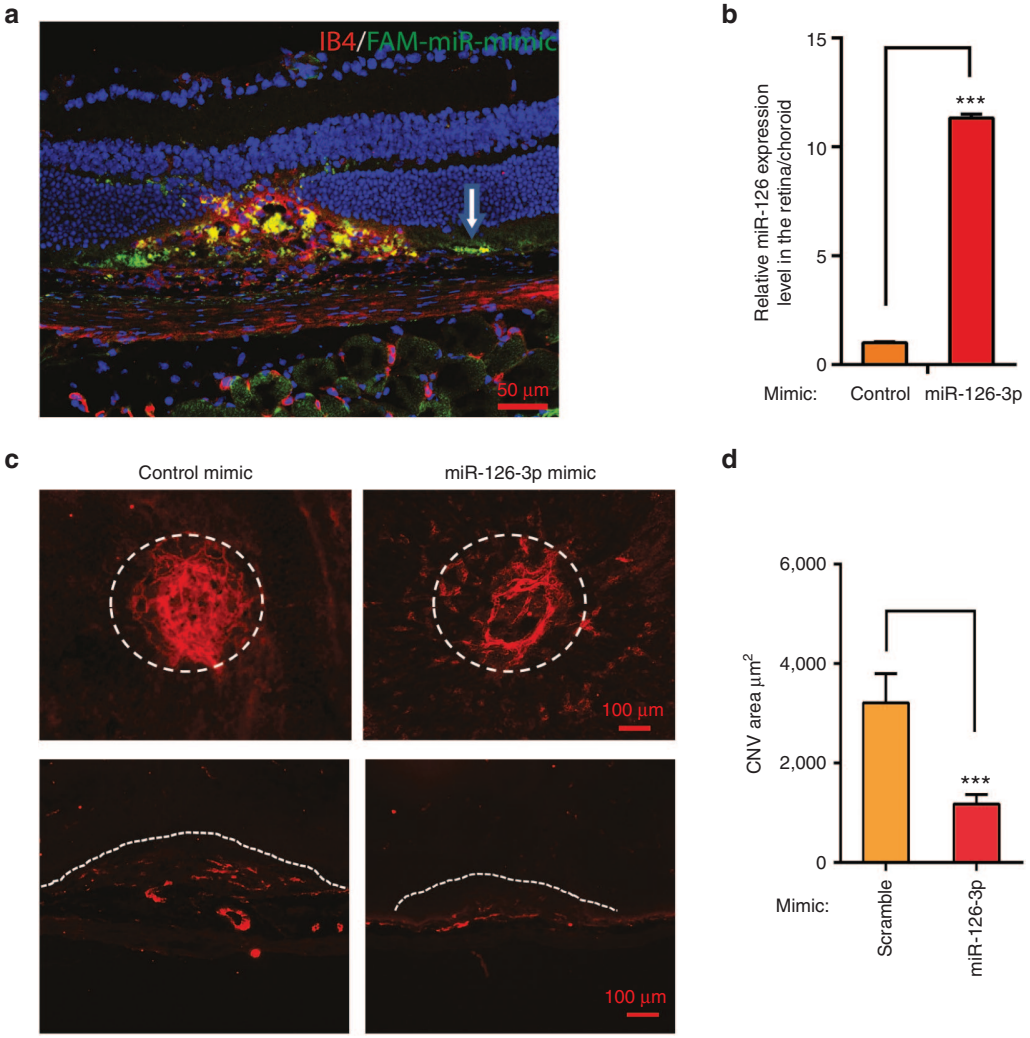

Figure 4 Repression of laser-induced CNV by miR-126-3p mimic *in vivo*. (**a**) Representative images of Isolectin-B4 staining at 3 days after laser injury subretinal injection of FAM labeled miRNA mimic. Note miRNA mimic taken up by RPE cells (white arrow) and choroidal vasculature (by IB4 and FAM co-staining) in the injured region. (**b**) Real-time PCR showing upregulation of miR-126-3p by miR-126-3p mimics in the posterior eyes. ***, $P < 0.001$. (**c**) Representative images after ICAM-2 staining showing repression of laser-induced CNV by miR-126-3p mimics compared to control mimics. Circled regions are the CNV areas. The bottom pictures show representative ICAM-2 staining of the injured regions after cross sectioning. miRNA mimic treatments were indicated and the lesion areas were labeled by dashed lines. Scale bar = 100 μm. (**d**) Quantification of CNV area (μm^2) in **c**. ***, $P < 0.001$.

affect VEGF-A expression, consistent with the strand-specific effect of miR-126 (Figure 6e). To further confirm whether miR-126 regulates VEGF level in RPE cells *in vivo*, RPE cells were isolated from *miR-126*$^{-/-}$ and WT control mice. By ELISA, Vegf-A protein secreted from the *miR-126*$^{-/-}$ RPE cells was significantly higher than that in WT controls, corroborating that miR-126 indeed regulates Vegf-A protein level *in vivo* (Figure 6f). Of note, *miR-126*$^{-/-}$ displayed defective angiogenesis in multiple organs (refs. [16,17] and Figure 2), suggesting that impaired VEGF signaling in ECs overrides the increased VEGF level in *miR-126*$^{-/-}$ mice. We also tested Vegf-A expression at 7 days after laser injury and miR-126-3p mimic injection by ELISA, and found miR-126-3p significantly represses Vegf-A expression in the laser-injured retina (Figure 6g). Together with our data that miR-126-3p mimic does not enhance angiogenic activity (Figure 5d,e), downregulation of VEGF by miR-126-3p mimic in RPE cells partially accounts for the reduced CNV after laser injury.

miR-126-3p regulates VEGF in RPEs cells by two distinct mechanisms

VEGF-A has been predicted by multiple miRNA target prediction programs, including PicTar, miRBase, miRanda, and Targetscan, to be a miR-126-3p target (Figure 7a). To further examine the mechanism that miR-126-3p directly targets VEGF-A, *VegfA* 3′-untranslated region (UTR) was amplified by RT-PCR from mouse lung cDNA, and cloned into pMIR-REPORT vector (Ambion). Co-transfection of pmiR-VegfA-UTR and miR-126 expressing plasmid was performed in 293T cells which show no endogenous miR-126 expression. Luciferase assay showed that ectopic overexpression of miR-126 strongly repressed VegfA 3′-UTR activity (Figure 7b). When mutations were introduced into miR-126 binding sequence in VegfA 3′UTR (ACGGUAC to UGCCAUG), the miR-126 repression effect was fully abolished. These results are consistent with recent reports, suggesting that VEGFA is a miR-126-3p target.[23,26] We also investigated

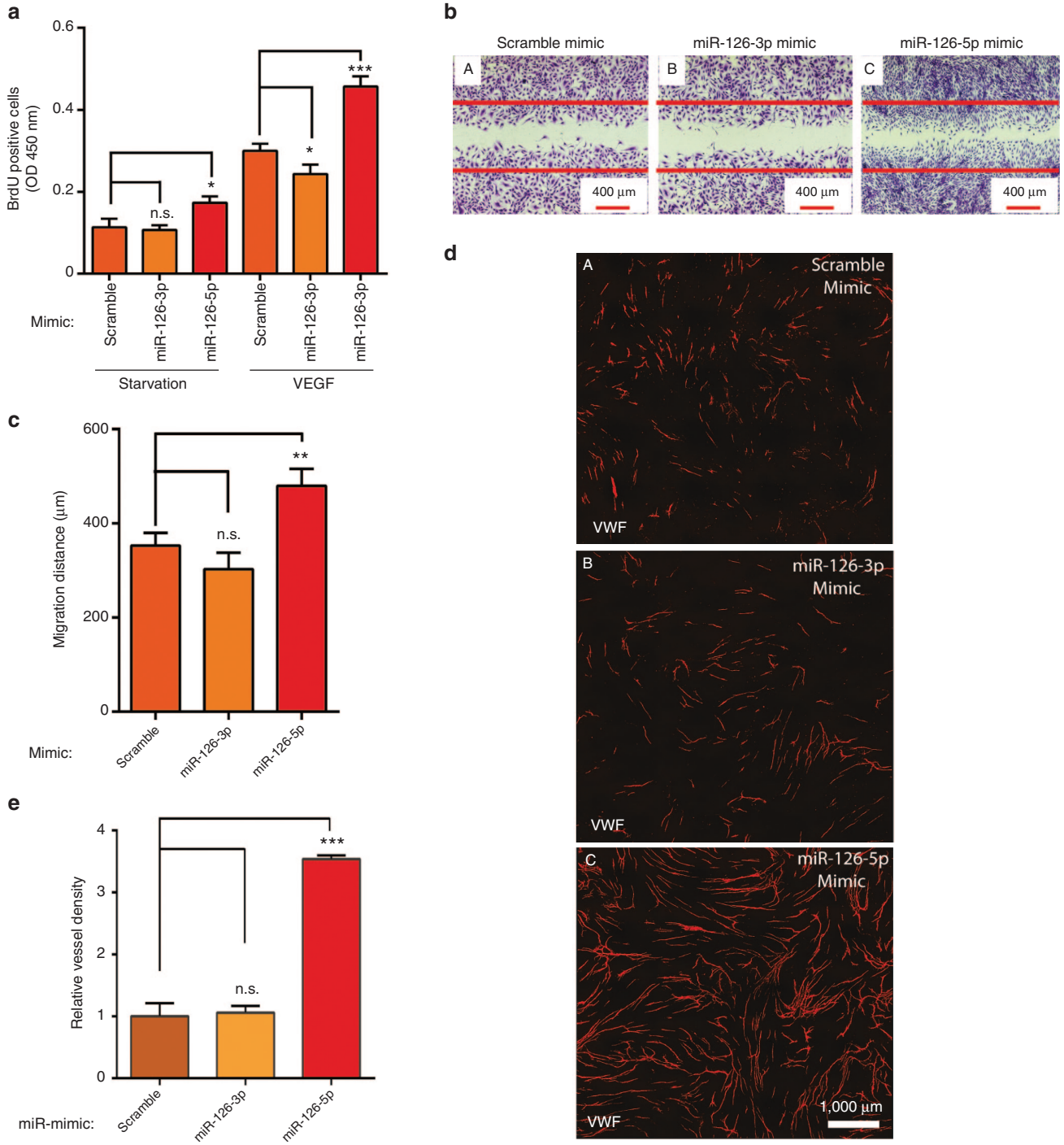

Figure 5 Promotion of angiogenesis by miR-126-5p but not miR-126-3p overexpression. (**a**) Quantification of EC proliferation in a BrdU incorporation assay under starvation and in response to VEGF after overexpression of miR-126-3p or miR-126-5p by miRNA mimics. *, $P < 0.05$; ***, $P < 0.001$. (**b**) Representative images of scratch wound EC migration after overexpression of miR-126-3p or miR-126-5p by miRNA mimics. The red lines label the initial position before VEGF treatment. Scale bar equals 400 μm. (**c**) Quantification of scratch wound EC migration after overexpression of miR-126-3p or miR-126-5p by miRNA mimics. N.S., not significant; **, $P < 0.01$. (**d**) Representative images of vessel-like structures as stained by antibody to vWF in an EC-fibroblast co-culture assay after overexpression of miR-126-3p or miR-126-5p by miRNA mimics in ECs. (**A**) Scramble control; (**B**) miR-126-3p mimic; (**C**) miR-126-5p mimic. Scale bar equals 1000 μm. (**e**) Quantification of EC-fibroblast co-culture assay after overexpression of miR-126-3p or miR-126-5p by miRNA mimics. **, $P < 0.01$; N.S., not significant.

additional mechanism that accounts for specific miR-126-3p function in RPE cells. RPE expression of αB-Crystallin (CryaB), a small heat shock protein, has been associated with drusen deposit during AMD progression.[32] It protects the denaturation and destabilization of proteins including VEGF by functioning as a chaperone protein.[33,34] We found that CryaB is also highly expressed in RPE cells compared to ECs (**Figure 7c**). Our microarray data showed that CryaB is significantly upregulated in ECs

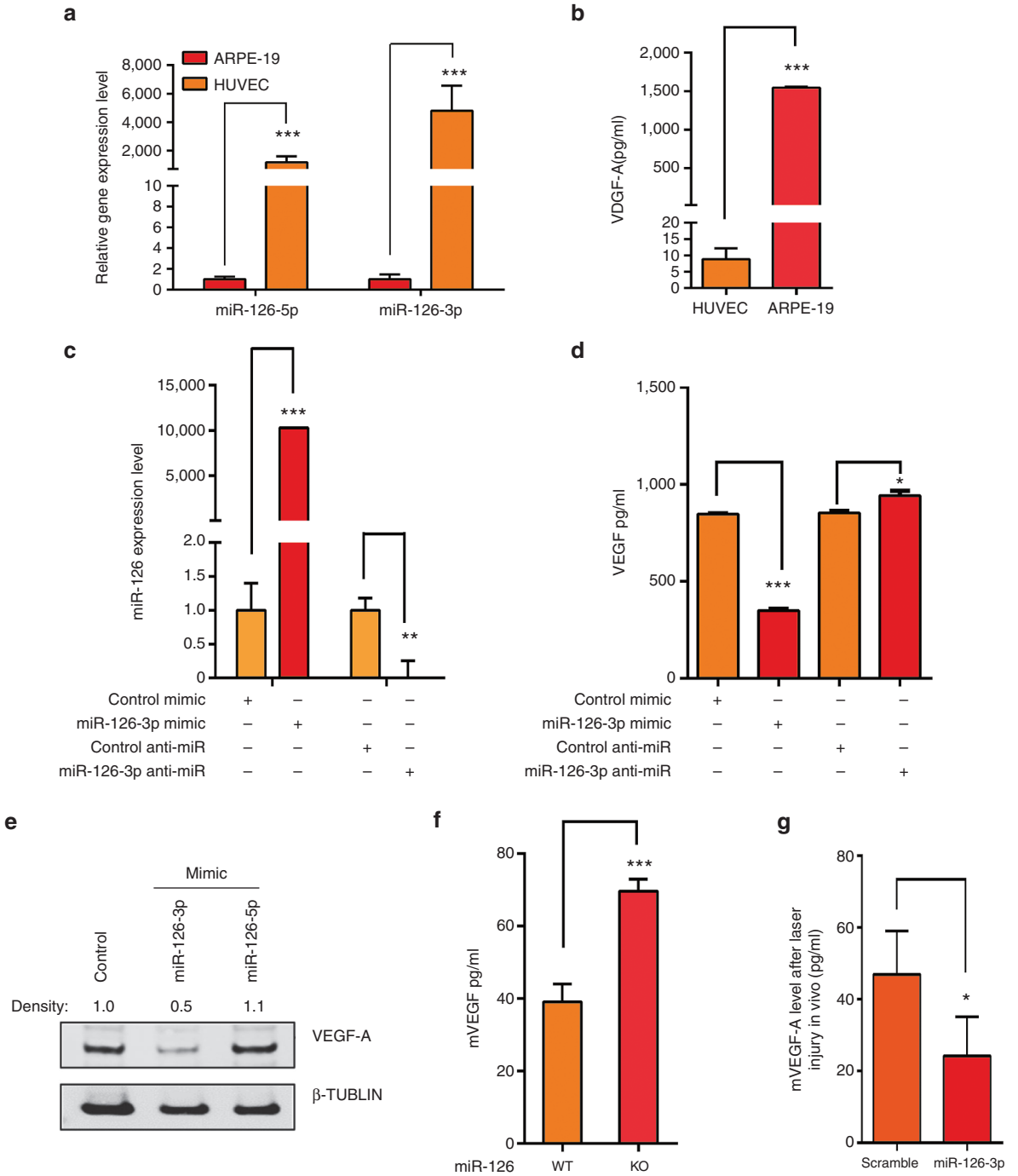

Figure 6 Regulation of VEGF expression by miR-126-3p in RPE cells. (**a**) Low expression of miR-126-3p and miR-126-5p in ARPE-19 cells compared to HUVECs as shown by qRT-PCR after normalized to U6. ***, $P < .001$. (**b**) Much higher secretion of VEGF-A by ARPE-19 cells compared to HUVEC cells as shown by ELISA analysis. ***, $P < 0.001$. (**c**) Upregulation and silencing of miR-126-3p in ARPE-19 cells by miR-126-3p mimic and LNA-modified antimiR, respectively. **, $P < 0.01$; ***, $P < 0.001$. (**d**) ELISA analyses showing regulation of VEGF-A by miR-126 mimic and anti-miR in ARPE-19 cells. *, $P < 0.05$; ***, $P < 0.001$. (**e**) Repression of VEGF-A by miR-126-3p but not miR-126-5p mimic in ARPE-19 cells as revealed by Western blot analysis. Density of the bands was noted. β-TUBULIN was used as control. (**f**) Elevated VEGF-A protein level as revealed by ELISA analysis in isolated *miR-126*$^{-/-}$ RPE cells compare to the WT RPE cells. (**g**) Repression of VEGF-A in the retina by miR-126-3p mimic injection after laser injury *in vivo*. *, $P < 0.05$.

isolated from *miR-126*$^{-/-}$ mice compared to WT mice.[17] Based on these, we hypothesized that miR-126-3p inhibits CryaB in RPE cells, which destabilizes factors including VEGF-A, and regulates CNV. Indeed, miR-126-3p mimic significantly decreased CryaB protein level, while LNA-modified miR-126-3p antimiR increased CryaB expression in ARPE-19 cells (**Figure 7d**). Moreover, we found both CryaB protein and RNA levels were elevated in RPE cells isolated from *miR-126*$^{-/-}$ mice compared to that in WT controls, supporting a causal role for miR-126 in regulating CryaB expression (**Supplementary Figure S6**). We also examined CryaB

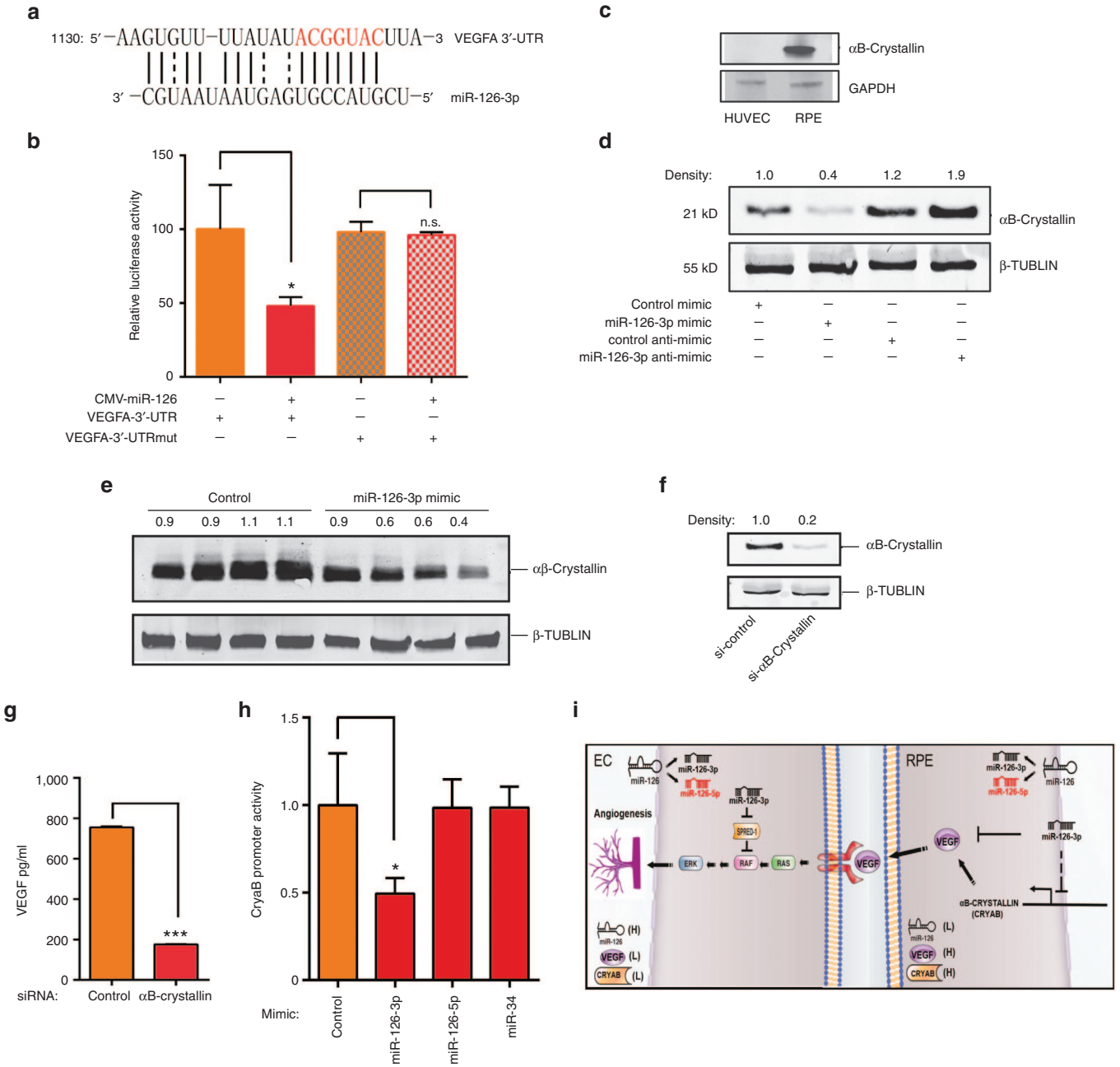

Figure 7 Two distinct mechanisms of VEGF regulation by miR-126-3p. (**a**) Sequence alignment of miR-126-3p with VEGFA 3′-UTR. (**b**) Repression of VEGF-A 3′-UTR activity by miR-126 in a luciferase reporter assay. For VEGF-A-3′-UTR mutant, the sequence complementary to the miR-126-3p seed region (labeled as red in **a** ACGGUAC was mutated to UGCCAUG. Note that VEGF-A mutant 3′-UTR doesn't respond to miR-126 repression. *, $P < 0.05$; NS, not significant. (**c**) Significantly higher expression of CryaB in ARPE-19 cells compared to HUVEC cells as shown by Western blot analysis. GAPDH was used as loading control. Density of the bands was noted. (**d**) Regulation of CryaB by miR-126-3p mimic and anti-miR in ARPE-19 cells as revealed by Western blot analysis. β-TUBULIN was used as loading control. Density of the bands was noted. (**e**) Repression of αB-Crystallin by miR-126-3p mimic in the RPE/choroid *in vivo* as revealed by Western blot analysis. β-TUBULIN was used as loading control. Density of the bands was noted. (**f**) Efficient silencing of αB-Crystallin by specific siRNA in RPE cells as shown by Western blot analysis. β-TUBULIN was used as loading control. Density of the bands was noted. (**g**) ELISA analysis showing downregulation of VEGF-A by αB-Crystallin silencing in ARPE-19 cells. ***, $P < 0.001$. (**h**) Repression of αB-Crystallin promoter activity by miR-126-3p but not miR-126-5p as shown by luciferase assay. miR-34 served as negative control. *, $P < 0.05$. (**i**) A model for cell type- and strand-specific function of miR-126 in ocular angiogenesis. Processing of miR-126 precursor generates miR-126-3p and miR-126-5p. miR-126 is highly expressed in EC cells, but lowly expressed in RPE cells. VEGF-A and CryaB show inverse relationship to miR-126 in expression in these two cell types. In ECs, inhibition of miR-126-3p represses angiogenesis partially by elevating the expression of *Spred-1*, a negative regulator of Ras/MAP kinase signaling. In RPE cells, over-expression of miR-126-3p represses VEGF by directly targeting VEGF and repressing CryaB promoter activity, therefore negatively regulates angiogenesis.

protein expression by Western blot analysis after laser injury and miR-126-3p mimic injection in mice, and found miR-126-3p mimic indeed significantly decreases CryaB protein level *in vivo* ($n = 4$, $P < 0.05$, Figure 7e). To determine whether downregulation of CryaB by miR-126-3p leads to decreased VEGF level, a specific siRNA was used to efficiently silence CryaB in ARPE-19 cells

(**Figure 7f**). By ELISA, silencing of CryaB significantly decreased level of secreted VEGF in RPE cells (**Figure 7g**). To further determine whether miR-126 represses CryaB transcription, we cloned a ~900 bp mouse CryaB promoter into the promoter-less luciferase reporter. By luciferase assay, miR-126-3p, but not miR-126-5p or nonrelevant miR-34, repressed CryaB promoter activity, suggesting that miR-126-3p represses CryaB expression through its promoter (**Figure 7h**).

DISCUSSION

Using mouse retina model, we provide genetic evidence that miR-126-3p, through its target gene *Spred-1*, plays a critical role in the development of retinal vascular layers. Moreover, we uncovered a strand and cell type-specific function for miR-126 in pathological angiogenesis. We found: (1) Silencing of anti-miR-126-3p by LNA-antimiR represses laser-induced CNV; (2) Overexpression of miR-126-3p by miRNA mimics also represses laser-induced CNV; (3) Overexpression of miR-126-5p but not miR-126-3p enhances angiogenesis in a EC-fibroblast co-culture assay; (4) miR-126-3p represses VEGF and CryaB expression in RPE cells. These indicate that miR-126 is required for proper angiogenesis, but the phenotype of miR-126 overexpression is dependent on cell types and the mature miR-126 strands (**Figure 7i**). Overexpression of miR-126-5p by mimics enhances angiogenesis in ECs, but overexpression of miR-126-3p in RPE cells represses angiogenesis through a noncell autonomous mechanism. These indicate an underappreciated cell type and strand-specific function of miR-126 in angiogenesis, suggesting the differential therapeutic effect of targeting miR-126-3p or -5p in angiogenesis-related disorders.

Cell type-specific function of miR-126 in angiogenesis and CNV

We confirmed the requirement of miR-126 in angiogenesis and found that *miR-126*$^{-/-}$ mice showed defective retinal vascular sprouting to the periphery region and into the intermediate and deep layers, a phenotype that can be partially rescued by knockout of its target gene *Spred-1 in vivo*. To our knowledge, our studies are the first to show that a miRNA is required for the development of intermediate and deep retinal vascular layers. Using an *in vitro* EC-fibroblast co-culture assay, we found silencing of miR-126-3p but not -5p represses angiogenesis, while overexpression of miR-126-5p but not -3p enhances angiogenesis, confirming the requirement and sufficiency of miR-126 in regulating angiogenesis.[15–17,19] Consistently, silencing of miR-126-3p represses but overexpression of miR-126-5p enhances laser-induced CNV. This result is consistent with the finding that silencing of miR-126 by antagomiR impares ischemia-induced angiogenesis.[18] We also found that overexpression of miR-126-3p represses laser-induced CNV, similar to what has been observed in an ischemia-induced retinal neovascularization model.[26] Similar phenotypes in leukemogenesis by overexpression and knockout of miR-126 has been reported recently.[35] We confirmed that miR-126-3p is highly enriched in the ocular ECs by ISH and by EC-enriched *miR-126/Egfl7* promoter activity. miR-126 is also expressed in the RPE cells at low level that is not detectable by ISH. To dissect the mechanism by which miR-126-3p mimic represses angiogenesis *in vivo*, we found overexpression of miR-126-3p but not miR-126-5p represses VEGF-A protein expression in RPE cells. VEGF-A from the RPE cells is one of the major drivers of pathological CNV in AMD patients. Indeed, VEGF level is upregulated in *miR-126*$^{-/-}$ RPE cells compared to that in WT controls, supporting an inverse causal relationship between miR-126 and VEGF-A in RPE cells. Under normal conditions, since miR-126 targets VEGF downstream signaling pathways, the EC sprouting angiogenesis is compromised in spite of this level of VEGF-A upregulation in RPE cells in *miR-126*$^{-/-}$ mice. However, likely because the miR-126 target sites in VEGF are not saturated by miR-126 in RPE cells under normal conditions, miR-126-3p overexpression has a dramatic effect in repressing VEGF-A expression in these cells. In ECs, miR-126 is required for proper angiogenesis by targeting *Spred-1*, which is supported by our genetic rescue experiments. The minimal effect of miR-126-3p mimic in EC angiogenic response could be explained by the saturation of miR-126-3p target genes including *Spred-1* in ECs under normal conditions.

Mechanistically, miR-126-3p regulates VEGF-A via two different mechanisms in RPE cells. One mechanism is miR-126-3p directly targets VEGF-A, as shown by our VEGF-A and VEGF-A mutant 5′UTR luciferase assays. These are consistent with previous publications.[23,26,36] The other mechanism relevant to AMD is miR-126-3p regulation of VEGF-A in RPE cells through a novel mechanism of repressing CryaB promoter activity. CryaB is a chaperone protein that can protect VEGF and other factors from denaturation and destabilization. Interestingly, both VEGF-A and CryaB are highly expressed in RPE cells in comparison to that in ECs, which is inversely correlated with the expression of miR-126. Our results reveal a cell type-specific function of miR-126 in angiogenesis, which should be seriously considered when interpreting miR-126 overexpression phenotype or designing miR-126-based therapeutics.

Distinct function of miR-126-3p and miR-126-5p in angiogenesis

Mouse miR-126 has two mature strands, miR-126-3p and miR-126-5p. Although knockout studies in mice have shown critical function of mouse miR-126 in angiogenesis, the strand-specific function of miR-126 in angiogenesis has not been sufficiently defined. We showed that silencing of miR-126-3p, but not miR-126-5p, represses angiogenesis an *in vitro* EC-fibroblast co-culture system. These results are consistent with our *in vivo* LNA-antimiR experiments that miR-126-3p silencing represses laser-induced CNV. In the miR-126 overexpression experiments, we found miR-126-5p but not miR-126-3p mimic enhances angiogenesis in EC-fibrolast co-culture assay, consistent with a recent report.[19] Consistently, we also found that miR-126-5p mimic increases laser-induced CNV. The difference of miR-126-3p and miR-126-5p in ECs could be accounted by their different target genes. When miR-126-3p is silenced, its target genes *Spred-1* and (*PIK3R2/p85-β*) are upregulated, which therefore represses angiogenic MAP kinase and PI3K signaling in response to angiogenic factors.[15–17,20] Overexpression of miR-126-3p does not further enhance angiogenesis in ECs probably because miR-126-3p target genes are saturated. In the RPE cells, which express low level of miR-126-3p but high level of miR-126-3p-regulated gene VEGF-A and CryaB, miR-126-3p

overexpression has a major impact in repressing the expression of VEGF-A, which signals to their neighboring ECs to repress angiogenesis. Our finding that miR-126-3p but not miR-126-5p represses CryaB promoter activity provides a novel mechanism for the distinct function of two miR-126 strands. How miR-126-3p regulates CryaB promoter activity is still unknown. Since CryaB can prevent the degradation of other growth factors, its regulation by miR-126-3p could provide additional mechanism beyond VEGF to explain its effect in repressing CNV.[37] miR-126-5p promotes EC proliferation by targeting NOTCH inhibitor *Dlk1*.[19] The complete mechanism for miR-126-5p in angiogenesis awaits future studies. In total, our studies highlight the differential function of different strands of a given miRNA, which could be dependent on the relative expression level of mature miRNA strands and their target genes.

Therapeutic implications

Anti-VEGF agents are being widely used to treat wet AMD. However, there is still great need for novel therapeutic target or agents to achieve better clinical outcome or circumvent drug resistance. Our findings that both miR-126-3p anti-miR and miR-126-3p mimic repress laser-induced CNV may have important implication in wet AMD. miR-126-3p anti-miR represses angiogenesis by repressing MAPK and PI3K-AKT pathways in response to angiogenic factors, while miR-126-3p mimic functions by targeting VEGF-A and regulating CryaB in RPE cells. Therefore, these agents may have significant therapeutic implications in treating wet AMD by different mechanisms. miR-126-3p regulates CryaB, which protects growth factors including VEGF from degradation and represents another therapeutic targets for AMD.[37] Of note, CryaB has been detected in the RPE of patients with early and advanced AMD,[38] while knockout of CryaB or CryaA inhibits pathological ocular neovascularization.[33,39] Upregulation of CryaB in ECs was shown to confer anti-VEGF resistance in cancer cells, suggesting that CryaB inhibition may function in addition to anti-VEGF in therapies.[40] Regulation of CryaB by miR-126-3p suggests that miR-126-3p may have therapeutic implications in other CryaB-related diseases than AMD, including cancer and neurodegenerative diseases. Although RPE cells from *CryaB*$^{-/-}$ mice shown increased death under oxidative stress, CryaB downregulation by miR-126-3p did not cause RPE cell death (**Supplementary Figure S7**), suggesting the safety of targeting CryaB using miR-126-3p mimic. We also found that miR-126-5p increases angiogenesis, consistent with a previous report.[19] This suggests that miR-126-5p may be beneficial in diseases with insufficient angiogenesis, such as limb or retinal ischemia. A therapeutic strategy that takes into account of the cell type and strand-specific function of miR-126 will be critical to achieve best outcome for miR-126-based therapy.

MATERIALS AND METHODS

Animals. Animal studies were conducted in accordance with the ARVO statement for the Use of Animals in Ophthalmic and Vision Research and were approved by the Institutional Animal Care and Use Committees at Tulane University. C57BL/6 male mice (6 to 8 weeks of age) were used for the studies in laser-induced CNV. *miR-126*$^{-/-}$ mice and their WT littermate controls were generated from *miR-126*$^{+/-}$ (backcrossed to C57BL6J background for 10 generations) breeding as described.[17] Generation of *miR-126/spred-1* double knockout mice was achieved by breeding *miR-126*$^{-/-}$ mice to *Spred-1*$^{-/-}$ mice.[27]

Eglf7/miR-126 promoter-LacZ transgenic mice were generated as described.[17] A 5.4kb mouse *Egfl7/miR-126* promoter was cloned into the hsp68 basal promoter upstream of a LacZ reporter gene, and was used for pronuclear injection. The primers for cloning are: 5′- TCAGGAAAAGAACTCAAGCTAAATTT-3′ and 5′-GCAATGCAACCTGCCCTTCCAG-3′. Two independent transgenic lines with similar LacZ expression pattern were used to characterize the promoter activity in the mouse eye.

miRNA mimics, LNA-anti-miRs, siRNAs, Laser-induced CNV and Retinal Vasculature staining. LNA-anti-miRs for miR-126-3p, miR-126-5p or scramble controls for *in vitro* were synthesized from Exiqon. miR-126-3p or control mimic for *in vitro* and *in vivo* studies were synthesized from Shanghai GenePharma Co. Sequence for control LNA-antimiR is: 5′- ACGTCTATACGCCCA-3′. Sequence for miR-126-3p LNA-antimiR is: 5′- TATTACTCACGGTACG-3′ Sequence for miR-126-5p LNA-antimiR is: 5′- CGTACCAAAAGTAATA-3′. Sequences for control mimic are: (sense) 5′-UUCUCCGAACGUGUCACGUTT-3′ and (antisense) 5′-ACGUGACACGUUCGGAGAATT-3′. Sequences for miR-126-3p mimic are: (sense) 5′- ucguaccgugaguaauaaugcg-3′ and (antisense) 5′-cgcauuauuacucacgguacga-3′. Sequences for miR-126-5p mimic are: (sense) 5′- cauuauuacuuuugguacgcg-3′ and (antisense) 5′-cguaccaaaaguaauaauguu-3′. siRNAs for human *αB-Crystallin* was purchased from Sigma. The sequences are as follows: human *αB-Crystallin* siRNA: 5′- CUGUGAAUGGACCAAGGAA(dT)(dT)-3′ and 5′- UUCCUUGGUCCAUUCACAG(dT)(dT)-3′.

Laser-induced CNV was induced in 6–8 week-old male C57BL/6J mice similarly as described using a murine Micron III system.[12] Briefly, animals were anesthetized with intraperitoneal injection of Ketamine (100 mg/kg) plus Xylazine (5 mg/kg). The pupils of anesthetized animals were dilated with 1% tropicamide (Alcon Laboratories, Forth Worth, TX), and a drop of topical analgesic (0.5% proparacaine) was applied. Gonak (2.5% hypromellose solution, Akorn, Lake Forest, IL) was then applied to both eyes. The eyes were imaged with a Micron III murine fundus camera (Phoenix Research Laboratories, Pleasanton, CA). Laser spots were applied using a Meridian Merilas 532 nm YAG laser (Thun, Switzerland) connected to the Micron III with a laser injector (Phoenix Research Laboratories). The Micron III laser injector only delivers ~15% of the energy to the eye, so the parameters were adjusted accordingly and the optimized conditions used were: 1,000 mW, 100 msec, and 100 μm spot size. Normally three to four evenly distributed laser spots were produced per eye, with the laser beam targeted at spots between major retinal vessels at a distance from the optic nerve head approximately three times the diameter of the optic disc. Formation of a bubble at the time of laser application indicates rupture of Bruch membrane and successful laser injury. Animals were injected subretinally with 1 μl of 200 ng/μl solution of miR-126-3p mimic or scramble control (GenePharma, Shanghai, China), or LNA modified miR-126-3p, miR-126-5p or scramble control antimiR (Exiqon) after laser photocoagulation. Two more injections were performed at day 4 to5 and 7 to 9 after injury. For visualizing the distribution of miRNA mimics, FAM-labeled miRNA was delivered at 7 days after laser injury, and the injected eyes were collected for flatmount imaging at 4 days after. At 14 days after laser injury, the treated eyes were fixed in 4% paraformaldehyde, and subjected to flatmount ICAM-2 staining or staining of frozen sections. For visualization of the retinal vasculature, retinas were dissected from pups or adult mice, and stained with Alexa-594 conjugated isolectin B4 (Molecular Probes, Thermo Fischer Scientific, Waltham, MA), PECAM-1 or ICAM-2 for retinal vasculature, and/or glial fibrillary protein for astrocytes. LacZ staining of the pmiR-126/*EGFL7-LacZ* retinas were performed using LacZ antibody (Abcam, Cambridge, MA). Images of CNV or retinal vasculature were captured using Nikon Eclipse Ti-S/L100 inverted microscope with fluorescence and cameras or a Nikon A1 Laser Scanning confocal microscope, and CNV volume were quantified using NIH ImageJ software.

RPE Cell isolation and culture. Human Retina Pigment Epithelium cell line (ARPE-19, ATTC CLR-2302) were cultured in DME/F-12 medium (HyClone GE healthcare, Logan, UT) supplemented with 10% FBS (HyClone) and 1× Penicillin-Streptomycin solution (HyClone) at 37 °C in 5% CO_2. The identity of ARPE-19 cells were confirmed by gene expression profile studies that will be published elsewhere. Mouse RPE cell isolation from WT and miR-126$^{-/-}$ mice was performed as described.[41] In brief, the anterior segment from each eye was removed and the neural retinas were carefully peeled away from the RPE-choroid-sclera. The eyecup was rinsed with Ca^{2+} and Mg^{2+} free 1xPBS (Gibco, Thermo Fischer Scientific, Waltham, MA) and treated with 0.25% trypsin (Gibco) for 1 hour at 37 °C. The trypsin was neutralized with DME/F12 1:1 medium (Gibco) supplemented with 20% FBS (Atlanta Biologicals, Flowery Branch, GA). Media was gently agitated to release mRPE into the media. The mRPE cells were cultured in DME/F12 1:1 medium supplemented with 20% FBS at 37 °C and 5% CO_2. After reaching confluence, the mRPE cells were subcultured in DME/F12 1:1 with 10% FBS at 37 °C and 5% CO_2. mRPE cells were characterized by RPE65 immunostaining and western blot (anti-RPE65, Santa-Cruz Biotechnology, Dallas, TX).

Plasmid construction and reporter assay. Mouse *αB-Crystallin* promoter was PCR amplified from mouse DNA and cloned into PGL3 Basic luciferase vector (Promega, Madison, WI). The sequences for the promoter cloning are: 5′- ATCGGGTACCACACCACCCAAAATAGTGCAGAGC -3′ and 5′- ATCGCTCGAGTGTGGCTAGATGAATGCAGAGTCG -3′. Reporter assays to test the promoter activities were performed after co-transfection with miR-126-3p, miR-126-5p, miR-34 or control mimics as described.[12] VEGF-A 3′ UTR and VEGF-A mutant 3′ UTR were directionally cloned into the pMIR-REPORT vector (Ambion). miR-126 expression plasmid cotransfection and reporter assays were performed as described.[17] Sequences for VEGF-A UTR cloning are: 5′-atcggagctc taatccagaaagcctgacatgaa-3′ and 5′-atcgaagctt cccccacaattattacggataaa-3′. In the VEGF-A UTR mutant, miR-126 binding sequence in VEGF-A 3′UTR was mutated from ACGGUAC to UGCCAUG by PCR-based mutagenesis.

EC proliferation, migration, and EC-fibroblast co-culture assays. For VEGF treatment, human umbilical vein endothelial cells (HUVECs) were starved with EC basal medium (EBM-2) with 0.1% FBS for overnight, and then treated with VEGF for the indicated periods of time. miRNA mimic or LNA-anti-miR transfection, and EC proliferation and migration in response to VEGF were performed as described.[13] For cell migration assay, 5-fluorouracil was added before VEGF treatment to prevent EC proliferation.

In vitro EC-Fibroblast co-culture was performed as described.[31] Briefly, human dermal fibroblast (HDF) cells were seeded into each well of a 12 well plate and maintained in DMEM with medium changes every 2–3 days until they developed confluent monolayers. HUVECs were maintained as described above and transfected with miR-126-3p, miR-126-5p or scramble control mimic or anti-miR at 1 day prior to seeding on HDF monolayers. Approximately 3×10^4 HUVECs were seeded onto each monolayer and the HDF/HUVEC co-culture was maintained for 7–14 days in EGM-2 medium with medium changes every 2–3 days to allow EC proliferation, migration, networking, and the formation of primitive vascular plexus. After 7–14 days the wells were fixed with 100% Methanol at −20 °C for 20 minutes and then stained with anti-VWF antibody (Dako, Carpinteria, CA) or PECAM-1 (BD Pharmingen, San Diego, CA). After hybridizing a secondary antibody, the endothelial tissue was visualized and imaged under a Nikon microscope. Multiple images were automatically stitched with Nikon software to provide a large image (several mm^2) and the resulting image was analyzed on ImageJ software to determine the degree of vascularization.

miRNA ISH. miR-126-3p ISH using LNA probe was performed as described.[42] Briefly, rehydrated mouse retina paraffin sections were treated with proteinase K, and hybridized with double digoxigenin (DIG)-labeled miR-126-3p probe (Exiqon, Denmark) in ISH buffer (50% Formamide, 5xSSC, 0.1%Tween, 9.2 mM citric acid for adjustment to pH6, 50 μg/ml heparin, 500 μg/ml yeast RNA). The sequence for the LNA probe is: gcattattactcacggtacga. After washing, the samples were incubated with anti-DIG antibody (1:800), and the signals were visualized by incubation with NBT/BCIP.

RNA, Western blot and ELISA analyses. Total RNA was isolated from mouse tissues or cell lines using TRIzol reagent (Invitrogen, Thermo Fischer Scientific, Waltham, MA). miRNA real-time RT-PCR was performed using qScript cDNA Synthesis and microRNA Quantification System (Quanta Biosciences, Beverly, MA). For Western blot analysis, protein lysates were resolved by SDS-PAGE and blotted using standard procedures. Antibodies used were as follows: αB-Crystallin (Cell signaling, Danvers, MA), Glyceraldehyde 3-phosphate dehydrogenase (Thermo Scientific) and β-Tubulin (Abcam) as loading control.

For Human and mouse VEGF ELISA, cells were treated with miRNA mimic or miRNA inhibitor for 48 hours in growth media, then change to base media without serum. The supernatants were collected after 24 hours in base media, centrifuged to remove all cell debris, and stored at −70 °C until analysis using ELISA kits (Human VEGF Quantikine ELISA Kit; R&D Systems, Minneapolis, MN) according to the methods recommended by the manufacturer. For ELISA of mouse tissue after laser injury, The posterior part of mice eyes were dissected and lysed by FastPrep-24 5G, immediately frozen in liquid nitrogen and stored at −70 °C before ELISA analysis for mouse VEGF.

Statistics. Each experiment was repeated at least three times. Student's *t*-tests were used to determine statistical significance between groups. *P*-values of less than 0.05 were considered to be statistically significant.

SUPPLEMENTARY MATERIAL

Figure S1. Relative expression level of miR-126-3p during retinal vascular development phenotype.
Figure S2. Retinal Vascular development phenotype in *miR-126*$^{-/-}$ mice.
Figure S3. Regulation of miR-126-3p after laser injury and *in vivo* efficiency of miR-126-3p and miR-126-5p antimiRs.
Figure S4. Enhancement of laser-induced CNV by miR-126-5p mimic.
Figure S5. miR-126-5p but not miR-126-3p mimetics represses DLK1 expression in HUVEC cells as shown by qRT-PCR. **, p<0.01.
Figure S6. Upregulation of aB-Crystallin at protein and mRNA levels in the RPE cells isolated from miR-126 knockout mice compared to that in WT control mice.
Figure S7. Unchanged RPE survival by miR-126 overexpression in RPE cells as shown by MTT assay.
Materials and Methods

ACKNOWLEDGMENTS

S.W. was supported by a Startup fund from Tulane University, NIH Grant EY021862, a career development award from the Research to Prevent Blindness foundation, and a BrightFocus Foundation Award in Age-related Macular Degeneration. Q.Z. was supported by an American Heart Association Southeast Affiliate Postdoctoral fellowship.

REFERENCES

1. Saint-Geniez, M and D'Amore, PA (2004). Development and pathology of the hyaloid, choroidal and retinal vasculature. *Int J Dev Biol* **48**: 1045–1058.
2. Stahl, A, Connor, KM, Sapieha, P, Chen, J, Dennison, RJ, Krah, NM *et al.* (2010). The mouse retina as an angiogenesis model. *Invest Ophthalmol Vis Sci* **51**: 2813–2826.
3. Jager, RD, Mieler, WF and Miller, JW (2008). Age-related macular degeneration. *N Engl J Med* **358**: 2606–2617.
4. Brown, DM, Kaiser, PK, Michels, M, Soubrane, G, Heier, JS, Kim, RY *et al.*; ANCHOR Study Group. (2006). Ranibizumab versus verteporfin for neovascular age-related macular degeneration. *N Engl J Med* **355**: 1432–1444.
5. Rosenfeld, PJ, Brown, DM, Heier, JS, Boyer, DS, Kaiser, PK, Chung, CY *et al.*; MARINA Study Group. (2006). Ranibizumab for neovascular age-related macular degeneration. *N Engl J Med* **355**: 1419–1431.
6. Zampros, I, Praidou, A, Brazitikos, P, Ekonomidis, P and Androudi, S (2012). Antivascular endothelial growth factor agents for neovascular age-related macular degeneration. *J Ophthalmol* **2012**: 319728.
7. Folk, JC and Stone, EM (2010). Ranibizumab therapy for neovascular age-related macular degeneration. *N Engl J Med* **363**: 1648–1655.
8. Krüger Falk, M, Kemp, H and Sørensen, TL (2013). Four-year treatment results of neovascular age-related macular degeneration with ranibizumab and causes for discontinuation of treatment. *Am J Ophthalmol* **155**: 89–95.e3.
9. Small, EM and Olson, EN (2011). Pervasive roles of microRNAs in cardiovascular biology. *Nature* **469**: 336–342.
10. Garofalo, M and Croce, CM (2011). microRNAs: Master regulators as potential therapeutics in cancer. *Annu Rev Pharmacol Toxicol* **51**: 25–43.
11. Wang, S and Olson, EN (2009). AngiomiRs–key regulators of angiogenesis. *Curr Opin Genet Dev* **19**: 205–211.

12. Zhou, Q, Gallagher, R, Ufret-Vincenty, R, Li, X, Olson, EN and Wang, S (2011). Regulation of angiogenesis and choroidal neovascularization by members of microRNA-23~27~24 clusters. *Proc Natl Acad Sci USA* **108**: 8287–8292.
13. Zhou, Q, Anderson, C, Zhang, H, Li, X, Inglis, F, Jayagopal, A *et al.* (2014). Repression of choroidal neovascularization through actin cytoskeleton pathways by microRNA-24. *Mol Ther* **22**: 378–389.
14. Sabatel, C, Malvaux, L, Bovy, N, Deroanne, C, Lambert, V, Gonzalez, ML *et al.* (2011). MicroRNA-21 exhibits antiangiogenic function by targeting RhoB expression in endothelial cells. *PLoS One* **6**: e16979.
15. Fish, JE, Santoro, MM, Morton, SU, Yu, S, Yeh, RF, Wythe, JD *et al.* (2008). miR-126 regulates angiogenic signaling and vascular integrity. *Dev Cell* **15**: 272–284.
16. Kuhnert, F, Mancuso, MR, Hampton, J, Stankunas, K, Asano, T, Chen, CZ *et al.* (2008). Attribution of vascular phenotypes of the murine Egfl7 locus to the microRNA miR-126. *Development* **135**: 3989–3993.
17. Wang, S, Aurora, AB, Johnson, BA, Qi, X, McAnally, J, Hill, JA *et al.* (2008). The endothelial-specific microRNA miR-126 governs vascular integrity and angiogenesis. *Dev Cell* **15**: 261–271.
18. van Solingen, C, Seghers, L, Bijkerk, R, Duijs, JM, Roeten, MK, van Oeveren-Rietdijk, AM *et al.* (2009). Antagomir-mediated silencing of endothelial cell specific microRNA-126 impairs ischemia-induced angiogenesis. *J Cell Mol Med* **13**: 1577–1585.
19. Schober, A, Nazari-Jahantigh, M, Wei, Y, Bidzhekov, K, Gremse, F, Grommes, J *et al.* (2014). MicroRNA-126-5p promotes endothelial proliferation and limits atherosclerosis by suppressing Dlk1. *Nat Med* **20**: 368–376.
20. Nicoli, S, Standley, C, Walker, P, Hurlstone, A, Fogarty, KE and Lawson, ND (2010). MicroRNA-mediated integration of haemodynamics and Vegf signalling during angiogenesis. *Nature* **464**: 1196–1200.
21. Tavazoie, SF, Alarcón, C, Oskarsson, T, Padua, D, Wang, Q, Bos, PD *et al.* (2008). Endogenous human microRNAs that suppress breast cancer metastasis. *Nature* **451**: 147–152.
22. Musiyenko, A, Bitko, V and Barik, S (2008). Ectopic expression of miR-126*, an intronic product of the vascular endothelial EGF-like 7 gene, regulates prostein translation and invasiveness of prostate cancer LNCaP cells. *J Mol Med (Berl)* **86**: 313–322.
23. Liu, B, Peng, XC, Zheng, XL, Wang, J and Qin, YW (2009). MiR-126 restoration down-regulate VEGF and inhibit the growth of lung cancer cell lines *in vitro* and in vivo. *Lung Cancer* **66**: 169–175.
24. Guo, C, Sah, JF, Beard, L, Willson, JK, Markowitz, SD and Guda, K (2008). The noncoding RNA, miR-126, suppresses the growth of neoplastic cells by targeting phosphatidylinositol 3-kinase signaling and is frequently lost in colon cancers. *Genes Chromosomes Cancer* **47**: 939–946.
25. Crawford, M, Brawner, E, Batte, K, Yu, L, Hunter, MG, Otterson, GA *et al.* (2008). MicroRNA-126 inhibits invasion in non-small cell lung carcinoma cell lines. *Biochem Biophys Res Commun* **373**: 607–612.
26. Bai, Y, Bai, X, Wang, Z, Zhang, X, Ruan, C and Miao, J (2011). MicroRNA-126 inhibits ischemia-induced retinal neovascularization via regulating angiogenic growth factors. *Exp Mol Pathol* **91**: 471–477.
27. Inoue, H, Kato, R, Fukuyama, S, Nonami, A, Taniguchi, K, Matsumoto, K *et al.* (2005). Spred-1 negatively regulates allergen-induced airway eosinophilia and hyperresponsiveness. *J Exp Med* **201**: 73–82.
28. Ryan, SJ (1982). Subretinal neovascularization. Natural history of an experimental model. *Arch Ophthalmol* **100**: 1804–1809.
29. Lanford, RE, Hildebrandt-Eriksen, ES, Petri, A, Persson, R, Lindow, M, Munk, ME *et al.* (2010). Therapeutic silencing of microRNA-122 in primates with chronic hepatitis C virus infection. *Science* **327**: 198–201.
30. Kleinman, ME, Yamada, K, Takeda, A, Chandrasekaran, V, Nozaki, M, Baffi, JZ *et al.* (2008). Sequence- and target-independent angiogenesis suppression by siRNA via TLR3. *Nature* **452**: 591–597.
31. Hetheridge, C, Mavria, G and Mellor, H (2011). Uses of the *in vitro* endothelial-fibroblast organotypic co-culture assay in angiogenesis research. *Biochem Soc Trans* **39**: 1597–1600.
32. De, S, Rabin, DM, Salero, E, Lederman, PL, Temple, S and Stern, JH (2007). Human retinal pigment epithelium cell changes and expression of alphaB-crystallin: a biomarker for retinal pigment epithelium cell change in age-related macular degeneration. *Arch Ophthalmol* **125**: 641–645.
33. Kase, S, He, S, Sonoda, S, Kitamura, M, Spee, C, Wawrousek, E *et al.* (2010). alphaB-crystallin regulation of angiogenesis by modulation of VEGF. *Blood* **115**: 3398–3406.
34. Liu, L, Qi, X, Chen, Z, Shaw, L, Cai, J, Smith, LH *et al.* (2013). Targeting the IRE1α/XBP1 and ATF6 arms of the unfolded protein response enhances VEGF blockade to prevent retinal and choroidal neovascularization. *Am J Pathol* **182**: 1412–1424.
35. Li, Z, Chen, P, Su, R, Li, Y, Hu, C, Wang, Y *et al.* (2015). Overexpression and knockout of miR-126 both promote leukemogenesis. *Blood* **126**: 2005–2015.
36. Ye, P, Liu, J, He, F, Xu, W and Yao, K (2014). Hypoxia-induced deregulation of miR-126 and its regulative effect on VEGF and MMP-9 expression. *Int J Med Sci* **11**: 17–23.
37. Kannan, R, Sreekumar, PG and Hinton, DR (2012). Novel roles for α-crystallins in retinal function and disease. *Prog Retin Eye Res* **31**: 576–604.
38. Alge, CS, Priglinger, SG, Neubauer, AS, Kampik, A, Zillig, M, Bloemendal, H *et al.* (2002). Retinal pigment epithelium is protected against apoptosis by alphaB-crystallin. *Invest Ophthalmol Vis Sci* **43**: 3575–3582.
39. Xu, Q, Bai, Y, Huang, L, Zhou, P, Yu, W and Zhao, M (2015). Knockout of αA-crystallin inhibits ocular neovascularization. *Invest Ophthalmol Vis Sci* **56**: 816–826.
40. Ruan, Q, Han, S, Jiang, WG, Boulton, ME, Chen, ZJ, Law, BK *et al.* (2011). αB-crystallin, an effector of unfolded protein response, confers anti-VEGF resistance to breast cancer via maintenance of intracrine VEGF in endothelial cells. *Mol Cancer Res* **9**: 1632–1643.
41. Yu, AL, Birke, K, Burger, J and Welge-Lussen, U (2012). Biological effects of cigarette smoke in cultured human retinal pigment epithelial cells. *PLoS One* **7**: e48501.
42. Jørgensen, S, Baker, A, Møller, S and Nielsen, BS (2010). Robust one-day in situ hybridization protocol for detection of microRNAs in paraffin samples using LNA probes. *Methods* **52**: 375–381.